

RESEARCH ARTICLE

Open Access



Long-term inhibition of Hepatitis B virus gene expression by a primary microRNA expressing ancestral adeno-associated viral vector

Njabulo Ziphezinhle Mnyandu¹, Shonisani Wendy Limani¹, Abdullah Ely¹, Reubina Wadee², Patrick Arbuthnot¹ and Mohube Betty Maepa^{1*}

Abstract

Current treatments for chronic infection with the hepatitis B virus (HBV) rarely cure carriers from the disease. Previously reported use of serotype 8 adeno-associated viral (AAV8) vectors to deliver expression cassettes encoding anti-HBV artificial primary microRNAs (apri-miRs) has shown promise in preclinical studies. A recently designed synthetic ancestral AAV (Anc80L65) with high liver transduction efficiency is a promising new addition to the anti-HBV vector toolbox. This study engineered Anc80L65 to express *HBx*-targeting apri-miRs. Single dose administration of the vectors to cultured cells and HBV transgenic mice effected reductions of secreted HBV surface antigen (HBsAg). Circulating HBV particles and HBV core antigen (HBcAg) were also significantly diminished in mice receiving the anti-HBV apri-miR-expressing ancestral AAVs. Downregulation of HBV biomarkers occurred over a period of 12 months. Absence of inflammatory responses or liver toxicity indicated that the vectors had a good safety profile. These data suggest that a single dose of apri-miR-expressing Anc80L65 is safe and capable of mediating durable suppression of HBV gene expression. Targeting *HBx*, which is required for transcriptional activity of covalently closed circular DNA of HBV, makes this Anc80L65-derived vector a promising candidate for functional cure from chronic HBV infection.

Keywords AAV, Ancestral AAV, Hepatitis B virus, MicroRNA

Introduction

Infection with hepatitis B virus (HBV) is endemic to sub-Saharan Africa, east and southeast Asia, and remains an important global health problem. It is estimated that ~300 million people are chronic carriers of the virus and at risk for complicating cirrhosis and liver cancer [1, 2]. Despite availability of an effective preventative vaccine, the global number of HBV-infected individuals is increasing and deaths resulting from persistent HBV infection are rising. The HBV replication intermediate comprising covalently closed circular DNA (cccDNA) is very stable, responsible for viral protein expression, and serves as template for synthesis of pregenomic RNA (pgRNA), which also encodes viral proteins, and viral

*Correspondence:

Mohube Betty Maepa
Betty.Maepa@wits.ac.za

¹Wits/SAMRC Antiviral Gene Therapy Research Unit, Infectious Diseases and Oncology Research Institute (IDORI), Faculty of Health Sciences, University of the Witwatersrand, Private Bag X3, Johannesburg Wits 2050, South Africa

²Department of Anatomical Pathology, School of Pathology, Faculty of Health Sciences, University of the Witwatersrand and National Health Laboratory Services, Johannesburg, South Africa



© The Author(s) 2025. **Open Access** This article is licensed under a Creative Commons Attribution-NonCommercial-NoDerivatives 4.0 International License, which permits any non-commercial use, sharing, distribution and reproduction in any medium or format, as long as you give appropriate credit to the original author(s) and the source, provide a link to the Creative Commons licence, and indicate if you modified the licensed material. You do not have permission under this licence to share adapted material derived from this article or parts of it. The images or other third party material in this article are included in the article's Creative Commons licence, unless indicated otherwise in a credit line to the material. If material is not included in the article's Creative Commons licence and your intended use is not permitted by statutory regulation or exceeds the permitted use, you will need to obtain permission directly from the copyright holder. To view a copy of this licence, visit <http://creativecommons.org/licenses/by-nc-nd/4.0/>.

protein-encoding mRNAs [3–5]. A single transcription termination signal located downstream of the HBV X protein encoding sequence (*HBx*) in the cccDNA results in *HBx* being present in all viral transcripts. The four HBV open reading frames (ORFs), *surface (S)*, *polymerase (P)*, *core (C)* and *HBx*, cover the entire cccDNA sequence in a very compact arrangement. In addition, *cis*-elements required for regulating transcription and reverse transcription are embedded in the protein coding sequences [6]. This compact arrangement, presence of the *HBx* sequence in all transcripts and important role of the encoded protein in regulating viral gene transcription [7], make *HBx* a good target for RNA interference (RNAi-) based therapy.

Licensed drugs for treating chronic HBV infection, which include derivatives of interferon-alpha and reverse transcription-inhibiting nucleoside and nucleotide analogs, effectively suppress viral replication but durable curative effects are rarely achieved [8–10]. Advancing new and effective anti-HBV therapy thus continues to be an important global priority. Persistence of extrachromosomal cccDNA is one of the main reasons for poor curative efficacy of currently licensed drugs, and a focus of research is developing strategies to reduce cccDNA content of hepatocytes in infected individuals. Although mechanisms responsible for formation and maintenance of cccDNA are incompletely understood, evidence indicates that *HBx* plays a central role, making it an attractive target for anti-HBV therapy development [7]. *HBx* interacts with several host factors to control gene expression from cccDNA and viral replication, with the interaction with DDB1-containing E3 ubiquitin ligase to destabilize viral restriction factors comprising the structural maintenance of chromosomes 5/6 (*Smc5/6*) complex well established [11]. Normally, *Smc5/6* complex inhibits transcription from extrachromosomal DNA, but degradation of this restriction factor enables viral gene expression and replication [12]. *HBx* has also been implicated in mediating viral immune evasion, persistence and carcinogenesis, by modulating interferon responses and facilitating HBV genome integration [11, 13].

Several studies have shown that HBV is susceptible to RNAi-mediated silencing. Both synthetic and expressed exogenous RNAi activators can reprogram the RNAi pathway and inhibit HBV replication in vitro and in vivo [14–16]. Chemically modified synthetic short interfering RNAs (siRNAs) against HBV, such as ARC-520 developed by Arrowhead Pharmaceuticals, are now in clinical trials and show promise [17, 18]. Although chemical modification of siRNAs enhances durability of viral gene silencing, it is not yet established whether the silencing is sufficiently lasting to be curative. Renewable transcription of RNAi activators produced from stable DNA

templates within HBV-replicating hepatocytes is thus appealing.

Expression cassettes encoding RNAi activators have the added advantage of compatibility with highly efficient recombinant viral vectors, such as recombinant adeno-associated viral (AAV) vectors. These thoroughly investigated vectors are safe and efficient for use in vivo [19–21]. To deliver expressed HBV-targeting RNAi activators, AAV8 has been widely used. The vector has excellent hepatotropism and gene silencers are expressed for a prolonged period [22, 23]. To advance hepatotropic vectors for gene therapy, bioinformatic analysis has been used to generate putative ancestral sequences, such as Anc80L65, that retain liver targeting but lack epitopes that feature on the capsid of AAV8 [24]. To evaluate utility of Anc80L65 for delivery of anti-HBV sequences, we have incorporated sequences that encode artificial primary microRNAs (apri-miRs) that use the scaffold of natural pri-miR-31 and contain a guide or multiple guides with cognates in the *HBx* ORF. Evaluation in cultured cells and in vivo demonstrates that the ancestral vectors are highly efficient and safe.

Methods

Plasmids encoding HBV genome targets, reporter gene or anti-viral sequences

Plasmids carrying the inverted terminal repeats (ITRs) and expressing apri-miRs targeting single or multiple coordinates of the *HBx* (pAAV31/5 or pAAV31/5,8,9 [22]) or multiple sites in the HCV genome (pBS-mTTRBCDE-pA [25]), were used to produce self-complementary AAVs (scAAVs). Plasmid pCH-9/3091, which carries greater-than-genome length of HBV [26], or psiCHECK-*HBx*, which bears the *HBx* sequence downstream of Renilla *luciferase* ORF and a separate Firefly *luciferase* expression cassette [27], were used to assay silencing of HBV targets.

Production and propagation of scAAVs

The scAAV vectors were produced using standard methods as previously described [24, 28–30]. Briefly, anti-HBV monocistronic (pri-miR 31/5), or polycistronic (pri-miR 31/5,8,9) apri-miRs were packaged into capsids of serotypes AAV2, AAV8 (Packaging plasmids kindly donated by Dirk Grimm, University of Heidelberg [30]) or Anc80L65 (Packaging plasmids kindly donated by Luk Vandenberghe, Harvard Medical School [24]) to produce scAAV2, scAAV8 or scAnc80 vectors (Fig. 1). Anti-HCV polycistronic apri-miR (mTTR BCDEpA) sequences were similarly packaged to produce control vector. AAVs were propagated in HEK293T cells by employing triple and quadruple transfection methods. Vectors were purified on an iodixanol gradient and titrated using quantitative PCR (qPCR). Viral genomes were purified from vector

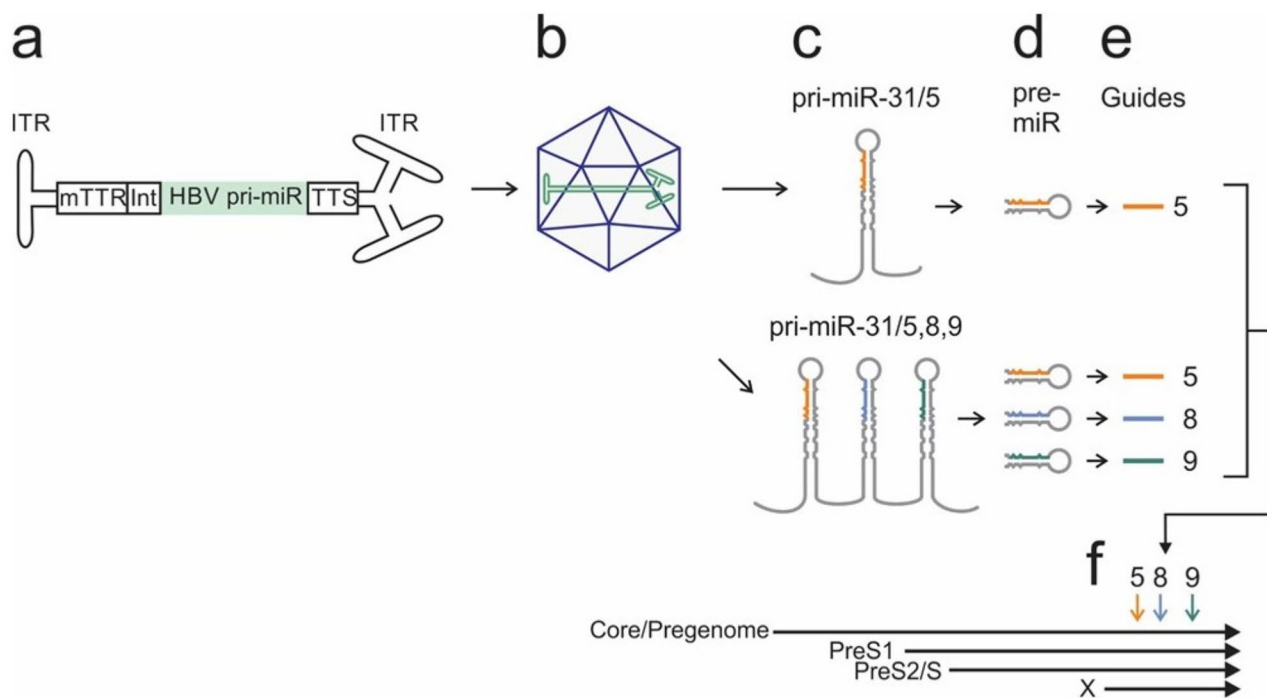


Fig. 1 Study design. **(a)** The scAAV vector genome was engineered to carry mono- or polycistronic artificial primary microRNA (apri-miR) sequences under control of a mouse transthyretin receptor (mTTR) promoter. ITR (inverted terminal repeats), int (intron) and TTS (transcription termination signal) are indicated schematically. **(b)** Engineered scAAV genomes were packaged into AAV2, AAV8 or Anc80L65 capsids. **c-f.** Upon administration, vectors mediate expression of pri-miRs **(c)** which are processed in several steps to generate pre-microRNA (pre-miR, **d**), and miR guides 5, 8 and 9 **(e)**. Produced miRs then target all four HBV transcripts (green, purple and orange arrows shows target sites **(f)**) (created with Biorender)

stocks using Qiagen's DNA and Blood mini kit (Qiagen, Hidden, Germany) and qPCR reactions carried out using Roche FastStart Essential DNA Green Master kit (Roche Applied Science, Penzberg, Germany) according to the manufacturer's instructions.

MTTR Forward (5' GCACTGGGAGGATGTTGAGT 3') and MTTR Reverse (5' CCCCTGTTCAAACATGT CCT 3') primers targeting mouse transthyretin receptor (mTTR) promoter sequence present in all recombinant AAV genomes were used for qPCR [22].

Measurement of HBV gene silencing in cultured cells

To evaluate inhibition of HBV gene expression in cultured cells, HepG2-hNTCP [31] or Huh7 lines were used. Huh7 cells were either transfected with 100 ng of a plasmid carrying HBV greater than genome length (pCH-9/3901 [26]), or a plasmid carrying *HBx* target sequence upstream of Renilla luciferase encoding sequence and a firefly luciferase encoding sequence in a separate cassette (psiCHECK-HBx [32]). Five hours post transfection scAAVs were administered to cells using an MOI of 10^5 . ELISA or Luciferase assay was performed 48 h after scAAV transduction according to the manufacturers' instructions using the Monalisa® Ag HBs Plus immunoassay kit (Bio-Rad, CA, US) or Dual-Luciferase® Reporter 1000 Assay System (Promega, WI, US) respectively.

HepG2-hNTCP cultures were infected with HBV at an MOI of 10 and incubated until the HBsAg ELISA reached an $OD_{490-655\text{ nm}}$ of 0.3. The cells were then infected with scAAVs at an MOI of 10^5 . Forty eight hours later, secreted HBsAg, VPEs, intracellular HBcAg and HBV RNA levels were assessed using Monalisa® Ag HBs Plus immunoassay, q-PCR, immunocytochemical staining and RT-qPCR respectively.

The qPCRs were carried out using Roche FastStart Essential DNA Green Master kit (Roche Applied Science, Penzberg, Germany) according to the manufacturer's instructions. HBV *surface* ORF-specific primers (HBVs-F and HBVs-R [33]) were used for DNA amplification. An AcroMatrix® HBV Panel (Thermo Fisher Scientific, CA, US) was used as the standards for quantification. To measure HBcAg, cells were fixed with cold methanol and immunohistochemical staining was performed using anti-HBV core antigen (HBcAg) primary antibody (Abcam, Cambridge, UK) and an Ultra-Sensitive ABC Peroxidase Staining Kit (Thermo Fisher Scientific, CA, US). All procedures were carried out according to the manufacturers' instructions and accredited guidelines.

RT-qPCR was performed to determine HBV transcript levels relative to *GAPDH* transcripts using previously described *surface* and human *GAPDH* specific primers [33]. RNA was extracted using Trizol™ Reagent

(Sigma, MO, US) from infected cells and Luna[®] Universal One-Step kit (New England BioLabs, MA, US) was used according to the manufacturer's instructions.

Detection of transgene expression from scAnc80 in vivo

HBV transgenic mice that carry replication competent greater-than-genome length HBV viral sequences were used for all in vivo studies following protocols approved by University of the Witwatersrand Animal Research and Ethics Committee [34]. To detect expression and processing of apri-miRs in vivo, 1×10^{11} VPEs of scAAVs were administered to 3 HBV transgenic mice per group via the tail vein. One or 12 months thereafter, livers were extracted for RNA isolation using Trizol[™] Reagent (Sigma, MO, US). Radioactively labeled probes were used to detect mature guides as has previously been described [22]. Northern blot hybridization analysis was performed on 45 µg of total liver RNA according to methods described previously [33]. Band intensities were quantified using ImageJ software [35].

Measurement of immune response induction markers in scAAV-injected mice

Inflammatory cytokine concentrations were measured in serum of mice at six hours after administration of 1×10^{11} scAAV VPEs per mouse. Each group comprised six mice and negative and positive controls received saline or an immunogenic poly (I: C) respectively. Cytokines, namely interleukin 6 (IL-6), interleukin 10 (IL-10), interleukin 12p70 (IL-12p70), interferon gamma (IFN-γ), monocyte chemoattractant protein-1 (MCP-1) and tumor necrosis factor-alpha (TNF-α) were analyzed using cytometric bead array (CBA) according to the manufacturer's instructions (BD Biosciences, CA, US). CBA reactions were processed with Fortessa FSR flow cytometer using BD FACSDiva software and data were analyzed with FCAP Array software 3.0 (BD Biosciences, CA, US).

Previously described methods were used to detect transcript concentrations of *interferon beta* (IFN-β), *Oligoadenylate synthase 1* (OAS-1) and *IFN-induced protein with tetratricopeptide repeats* (IFIT-1) relative to murine *glyceraldehyde-3-phosphate dehydrogenase* (mGAPDH) [33]. Livers from a group of 4 mice were harvested 6 h after AAV injection, and RNA extracted using Trizol[™] Reagent (Sigma, MO, US). To perform mRNA quantification, RT-qPCR was carried out using Luna[®] Universal One-Step kit (New England BioLabs, MA, US) according to the manufacturer's instructions.

Determination of HBV gene silencing in mice

To assess HBV gene silencing inhibition in mice, eight mice per group were injected via the tail vein with either scAAV vectors at 1×10^{11} VPEs/mouse or saline. Serum samples were harvested over a 12-month period. HBsAg

expression was measured in 50× diluted serum samples using the Monalisa[®] Ag HBs Plus immunoassay kit (BioRad, CA, US). To quantify circulating HBV VPEs in transgenic mice, HBV genome copy numbers were quantified by qPCR as described above. To measure intrahepatic HBcAg, 3 mice per group were sacrificed at 1 or 12 months after scAAV administration and livers fixed in 10% neutral buffered formalin (Sigma, MO, US). Fixed liver tissues were processed by the National Health Laboratory Services (NHLS, Johannesburg, South Africa) using accredited procedures and HBcAg staining was performed as above.

RT-qPCR was performed to determine HBV transcript levels relative to *GAPDH* transcripts using previously described *core* and mouse *GAPDH* specific primers [33]. RNA extracted using Trizol[™] Reagent (Sigma, MO, US) from livers harvested from a group of 4 mice at 1 and 12 month post AAV injection and Luna[®] Universal One-Step kit (New England BioLabs, MA, US) was used according to the manufacturer's instructions.

Evaluation of scAAV-induced liver toxicity in mice

Elevation of alanine transaminase (ALT) activity is specific for liver toxicity and was measured in serum samples harvested from 3 mice per group over an 8-week period following scAAV injection. Samples were processed in the accredited facilities of the South African NHLS (Johannesburg, South Africa) using an Advia 1800 Chemistry System. To assess infiltration of inflammatory cells and fibrosis, sections from livers harvested at 1- or 12-months post scAAV administration were stained with hematoxylin and eosin (H&E) or Sirius red according to approved methods (NHLS, Johannesburg, South Africa).

Statistical analysis

Data are expressed as standard error of mean. GraphPad Prism software (GraphPad Software Inc, CA, USA) was used to perform one-way ANOVA or Student's two-tailed paired t-test or Tukey's multiple comparison test where *p* values < 0.05 (*), < 0.001 (**), < 0.0001 (***) were regarded as statistically significant.

Results

The scAnc80 vector mediates HBV gene knockdown in cultured cells

The integrity of plasmids used in AAV production was confirmed by restriction map analysis which showed expected banding patterns (Figure S1). To assess the effects of scAnc80 on HBV gene expression in vitro, Huh7 cells were transfected with psiCHECK-HBx or pCH-9/3901 before transduction with scAAVs expressing mono or polycistronic anti-HBV or anti-HCV apri-miR at MOIs of 10^5 . Luciferase assays were performed on lysates of psiCHECK-HBx-transfected cultures 48 h

post transduction with either scAAV2 miR-31/5, scAAV2 miR-31/5,8,9, scAnc80-31/5 or scAnc80 miR-31/5,8,9, which showed decreases in *Renilla* luciferase activity relative to controls, confirming that the miRs specifically target the *HBx* sequence (Fig. 2a). Vectors carrying polycistronic anti-HBV apri-miR performed better than vectors carrying monomeric apri-miR. HBsAg measured in supernatants of Huh7 cultures that had been transfected with pCH-9/3901 then transduced with scAAVs corroborated results using the psiCHECK-HBx reporter. Again, vectors carrying polycistronic anti-HBV apri-miRs performed slightly better than vectors carrying monomeric apri-miR (Fig. 2b).

To model HBV infection in humans more closely, the hNTCP-HepG2 cell line was infected with HBV at an MOI of 10 before infection with scAAVs at an MOI of 10^5 . Forty eight hours after scAAV administration, ELISA showed a reduction in HBsAg concentrations relative to negative controls. However, the differences between HBsAg values following administration of vectors carrying polycistronic anti-HBV apri-miR and those carrying monomeric apri-miR were not statistically significantly different (Fig. 2c). Further validating the efficacy of the vectors against HBV is the reduction in secreted HBV particles (Fig. 2d), HBV RNA (Fig. 2e) and HBcAg (Fig. 2e) levels in hNTCP-HepG2 cells infected with apri-miR expressing scAAV2 and scAnc80

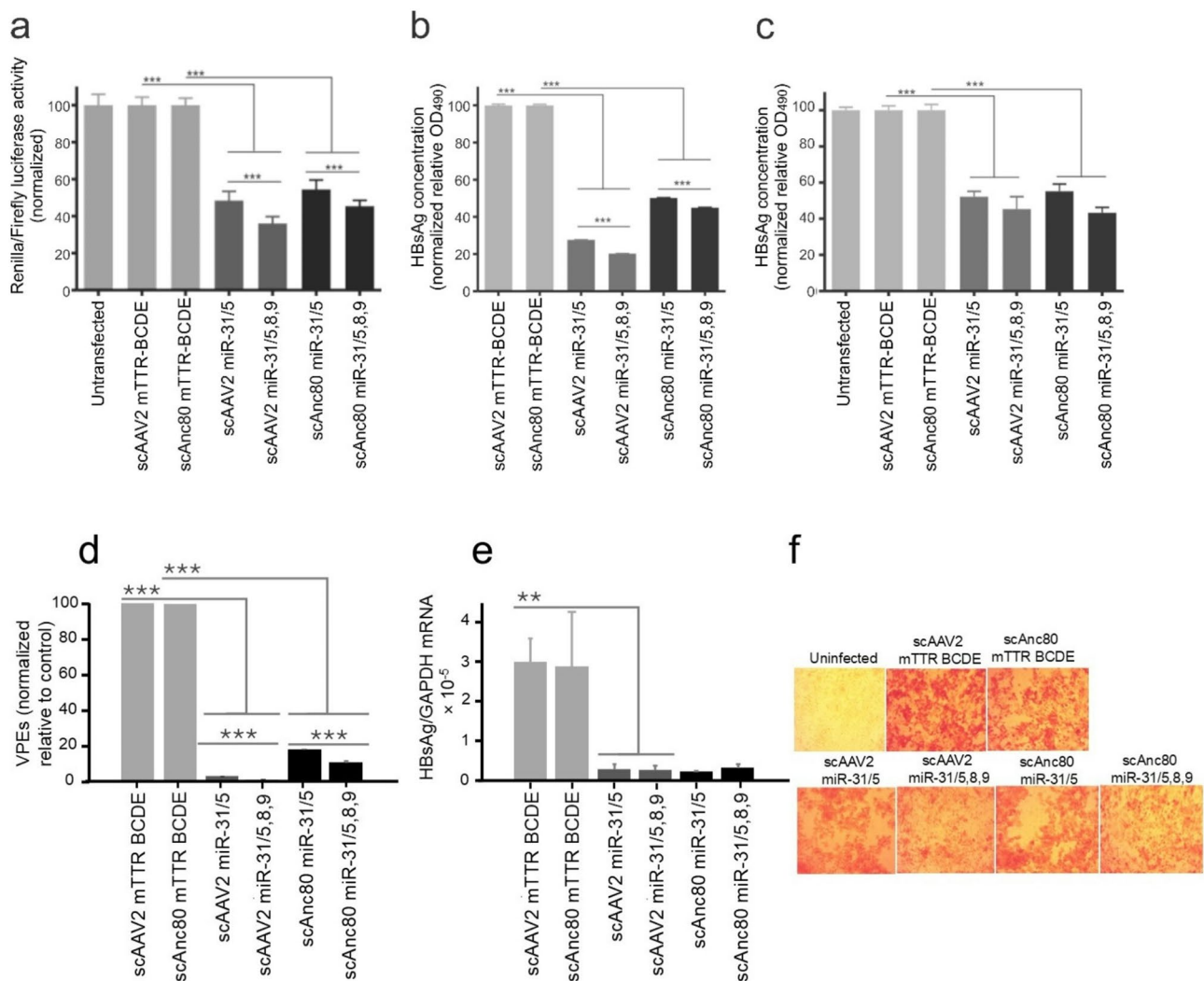


Fig. 2 Assessment of scAAV activity in culture. **a**. Assessment of HBV gene expression knockdown by scAAV vectors following transfection of Huh7 cells with psiCHECK-*HBx*. Data are represented as a mean ratio of *Renilla* to Firefly Luciferase reporter activity. **b**. Transfection with pCH 9/3901 then transduction with scAAVs was performed before measurement of HBsAg. **c-f**. Evaluation of HBsAg (**c**), secreted HBV viral particle equivalents (**d**, VPEs), intracellular HBV RNA (**e**) and HBcAg levels in HepG2-hNTCP cells infected with HBV and then transduced with scAAVs. Data shown are relative to control vectors encoding anti-HCV apri-miRs. The means (\pm SEM) were derived from $n = 3-4$ samples. The Student's two-tailed paired t-test or Tukey's multiple comparison test was used to ascertain statistically significant differences relative to controls. p values < 0.05 (*), < 0.001 (**), < 0.0001 (***) were regarded as statistically significant

as compared to negative controls. Similarly, vectors carrying polycistronic anti-HBV apri-miR performed better than vectors carrying monomeric apri-miR in reducing HBV VPEs. Although a decrease in HBV levels by scAnc80 vectors was observed, it was not statistically significant. Although AAVs transduce liver-derived cell lines inefficiently [36, 37], and anti-HBV effects are lower than silencing following transduction with adenoviral vectors bearing the same cassettes [22, 38], these data indicate that scAnc80 transduces cells in vitro and reduce HBV gene expression.

scAnc80 administration mediates a prolonged transgene expression in vivo

To confirm activation of the RNAi pathway in HBV transgenic mice following scAAV administration, Northern blot hybridization analysis was performed on RNA extracted from liver homogenates prepared at 1 or 12 months after mice received the AAVs. Probes complementary to guide sequences 5, 8 or 9 were used to detect mature miRs. The guide 5 sequence was detected in all mice treated with scAAVs carrying pri-miR 31/5 or pri-miR 31/5,8,9 and showed abundance at both time points of analysis. As expected, guide 8 sequence was only detected in extracts from mice that were treated with scAAVs carrying polycistronic pri-miR 31/5,8,9. However, because of low-level production of the guide 9 sequence, it was undetectable in mice receiving scAAVs expressing miR-31/5,8,9 (Fig. 3, S2). This observation is

in accordance with previously reported data showing that processing of individual pri-miR is affected by its position within a polycistronic pri-miR [22, 32]. High molecular weight bands representing unprocessed pri-miRs or pre-miRs were also observed (Figure S2). Supported by 12 months hepatic stability of scAAV genomes (Figure S3), these results show that scAnc80 vectors achieve an impressive long-term hepatic transgene expression, which was still detectable a year after single dose AAV injection.

scAnc80 mediates downregulation of HBV genes in transgenic mice

To assess ability of scAnc80s to reduce HBsAg in vivo, HBV transgenic mice were injected with anti-HBV scAAVs or vector controls. ELISA analysis performed at regular time points for the 12-month duration of the experiments revealed a significant and sustained decline of HBsAg by about 80% 90% in mice receiving scAAVs carrying anti-HBV apri-miRs. Notably, efficacy of scAnc80 and scAAV8 vectors carrying apri-miRs was similar. With both vectors, HBsAg concentrations were reduced as early as 2 weeks until 12 months after vector administration (Fig. 4a, S4a). Quantification of circulating HBV particle equivalents showed a significant decline at 1 month after injection with anti-HBV apri-miR-expressing vectors. The viral particle reduction achieved at 1 month by scAnc80 was similar to that achieved by scAAV8 vectors. The HBV load showed a sustained

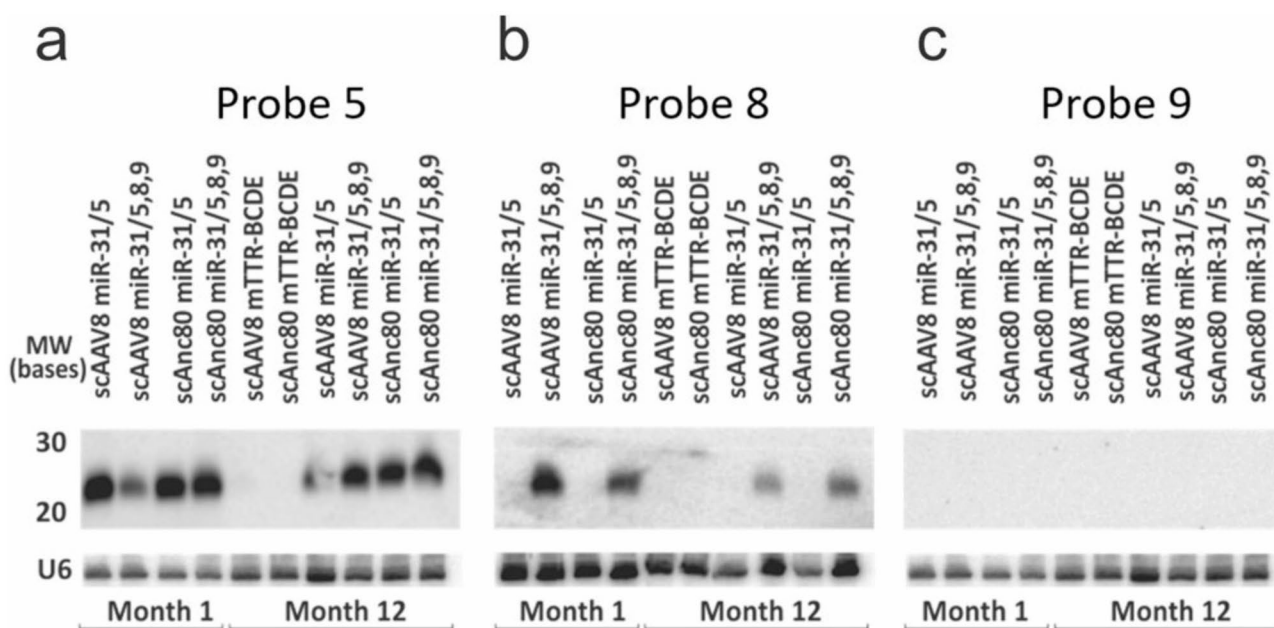


Fig. 3 Expression and processing of artificial primary microRNA from scAnc80. Northern blot hybridization was performed on total RNA extracted from murine liver samples at 1 or 12 months post infection with scAAVs using probes complementary to sequence for guides (a) 5, (b) 8 or (c) 9. The figure shows data from a representative of 3 mice per group. After stripping miR probes from the blots, rehybridization with a probe complementary to U6 small nuclear RNA probe was carried out to confirm equal loading. MW, molecular weight

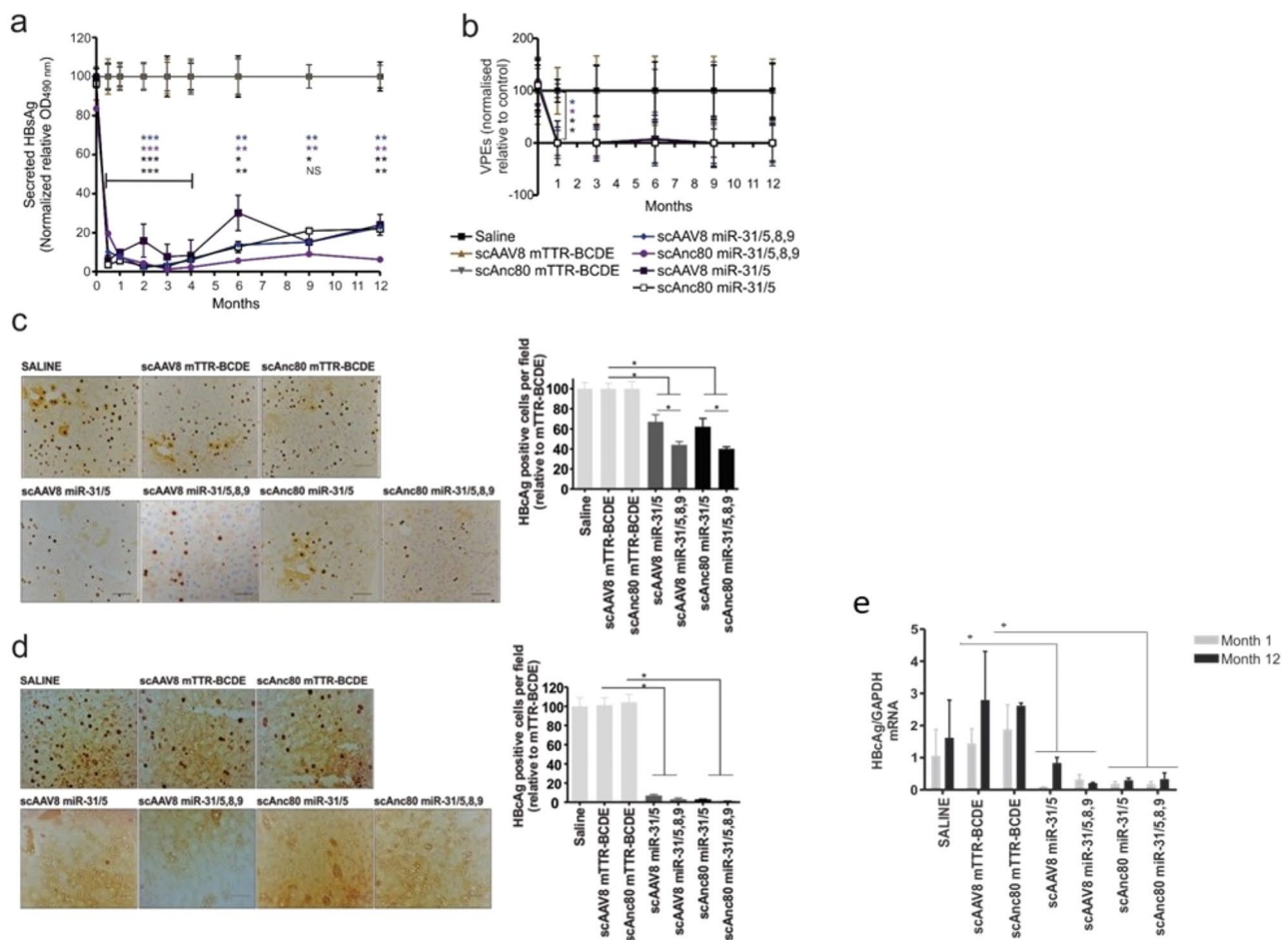


Fig. 4 HBV gene silencing in transgenic mice. Eight HBV transgenic mice per group were injected intravenously with saline or 1×10^{11} scAAV genome copies. **a.** Serum HBsAg and **(b)** HBV particles were measured over a 12-month period using ELISA or qPCR respectively. Immunohistochemical staining was performed on mouse liver sections at **(c)** 1 or **(d)** 12 months post scAAV infection. Liver sections from a representative of 3 mice per group taken at 20 \times magnification are shown. Graphs on the right show quantification of HBcAg-positive cells (brown) from 10 randomly selected fields per group. All values were normalized and presented relative to anti-HCV vectors. **e.** HBV transcript levels relative to *GAPDH* transcripts determined using RT-qPCR. RNA was extracted from livers harvested from 4 mice per group at 1 and 12 month post AAV injection. The means (\pm SEM) were derived from groups comprising 4 to 6 mice. One-way ANOVA was used to ascertain statistically significant differences relative to anti-HCV vector controls. *p* values < 0.05 (*), < 0.001 (**), < 0.0001 (***) were regarded as statistically significant

downward trend over the remainder of the 12-month period and HBV VPEs were not significantly different in mice receiving scAnc80 or scAAV8 vectors (Fig. 4b, S4b).

Immunohistochemistry to detect HBcAg was performed on liver samples from mice sacrificed at 1- or 12-months post administration of scAAV. These data revealed intrahepatic HBcAg levels that were significantly diminished in animals receiving the anti-HBV apri-miRs compared to controls (Fig. 4c, d). As with observations using cultured cells, the scAnc80 and scAAV8 vectors carrying polycistronic anti-HBV apri-miRs performed better than vectors carrying monomeric apri-miRs. At 1 month after AAV injection, vectors carrying the trimeric apri-miRs achieved about 50% HBcAg reduction, which was greater than the 35% reduction achieved by monomeric apri-miRs (Fig. 4c). However, efficacy at 12 months

was more impressive, and all scAAVs carrying anti-HBV apri-miRs showed HBcAg reduction of more than 95% (Fig. 4d). This improved reduction in silencing efficiency at 12 months, as compared to inhibition at 1 month, was not observed with other HBV replication markers. Although these differences are difficult to explain, they may be related to the variance in the half-life and assay procedures used to measure the viral replication markers [39–41]. To validate HBV transcripts' targeting by scAnc80 vectors, HBV RNA levels were determined at 1 and 12 months post AAV infection. As expected, significant reduction of HBV transcripts was observed at 1 month and similar trends were observed at 12 months post injection with AAVs (Fig. 4e). Taken together, these results demonstrate that scAnc80 mediates long-term HBV gene suppression. These observations are consistent

with persistence of scAAVs genomes in hepatic tissue (Figure S3) and long-term expression of transgenes (Fig. 3, S2).

Inflammatory response markers are not affected by administration of scAnc80

To quantify serum concentrations of pro-inflammatory cytokines (IL-6, IL-10, IL-12p70, IFN- γ , MCP-1, and TNF- α), CBA was performed at 6 h after scAAV administration. In groups of mice receiving these vectors concentrations of all cytokines, with the exception of MCP-1, were similar to those detected in mice injected with saline (Fig. 5a-f, S5). The increase in MCP-1 was modest for anti-HBV pri-miRs expressing scAAV8. Although this modest MCP-1 elevation is difficult to explain, it is not significant for scAnc80 vectors and is in contradiction with previous studies using these pri-miRs, hence it cannot be attributed to pri-miR expression [22]. As expected, immunogenic poly (I: C) elevated most cytokines except IFN- γ and IL12p70. Evaluation of the activation of IFN response genes was performed using RNA

extracted from hepatic tissue homogenates that were harvested 6 h after saline, poly (I: C) or scAAV administration. Titration of RNA from *IFN- β* and its associated *IFIT-1* and *OAS-1* genes revealed similar expression levels in mice injected with saline or scAAVs (Fig. 5g-i). Poly (I: C) induced significant *IFIT-1* expression, but *IFN β* and *OAS-1* were not similarly affected. Collectively, these findings indicate that scAnc80 administration does not induce a pro-inflammatory response in mice.

Administration of scAnc80 does not induce hepatic injury

Histological evaluation was carried out on hepatic tissue extracted from mice at 1 or 12 months after AAV injection. Although H&E staining revealed mild inflammation in groups of mice injected with scAAVs, the same observation was made in groups of mice receiving saline (Fig. 6a). The source of inflammation could therefore not be linked to scAAV infection. In addition, staining with Sirius red revealed no signs of tissue fibrosis in mice receiving scAAVs or saline (Fig. 6b). To eliminate any possibility that expression of apri-miR from scAnc80 in HBV

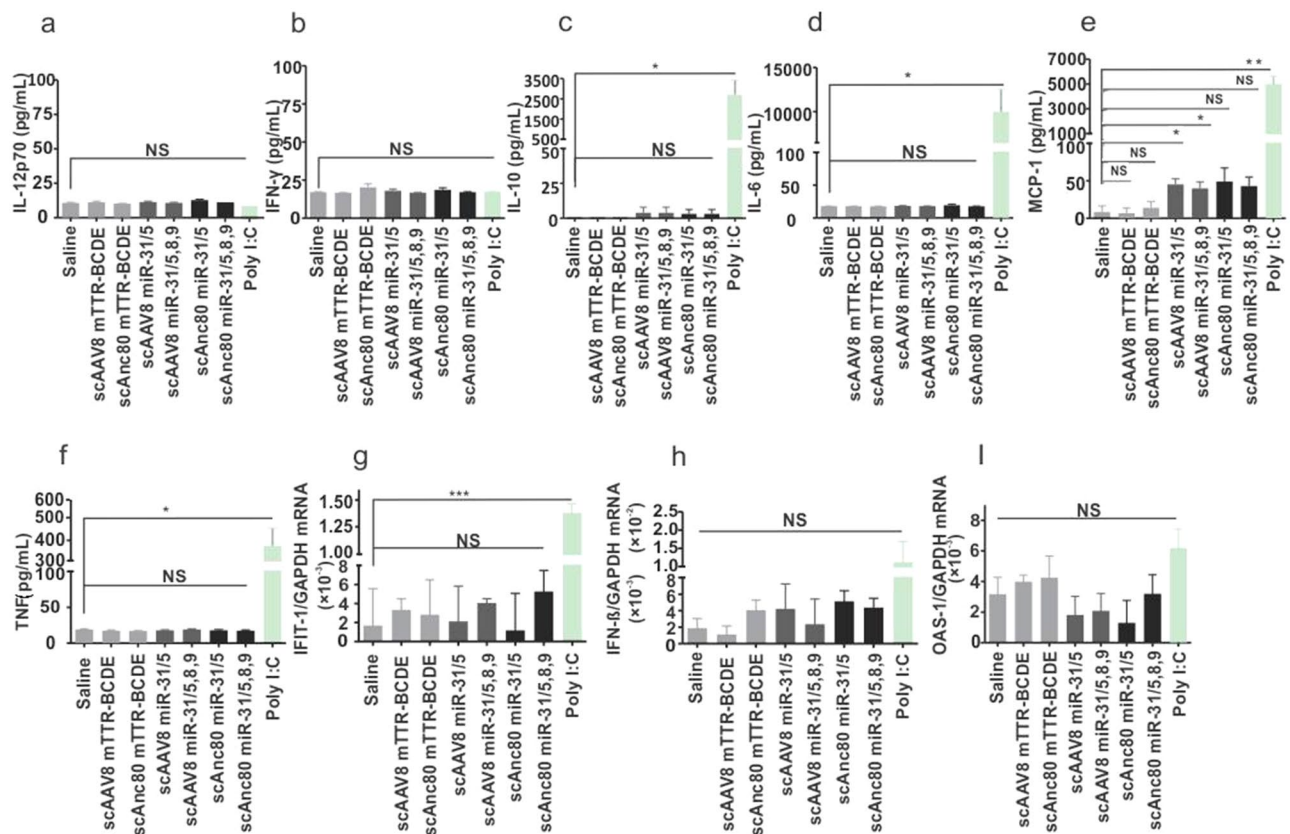


Fig. 5 Measurement of pro-inflammatory response in scAnc80 infected mice. Cytokine quantification was performed 6 h after injection with scAAVs, saline or poly (I: C). Cytometric bead array assay quantification of serum cytokines from 6 mice per group: (a) IL-12p70, (b) IFN- γ , (c) IL-10, (d) IL-6, (e) MCP-1 and (f) TNF- α . Concentrations of (g) *IFIT-1*, (h) *IFN- β* , (i) and *OAS-1* mRNAs in liver samples from 4 mice per group determined using RT-qPCR. The means (\pm SEM) were derived from six or four mice per group. The Student's two-tailed paired t-test was used to ascertain statistically significant differences relative to the saline control. *p* values < 0.05 (*), < 0.001 (**), < 0.0001 (***) were regarded as statistically significant and *p* values \geq 0.05 were regarded as statistically insignificant (NS)

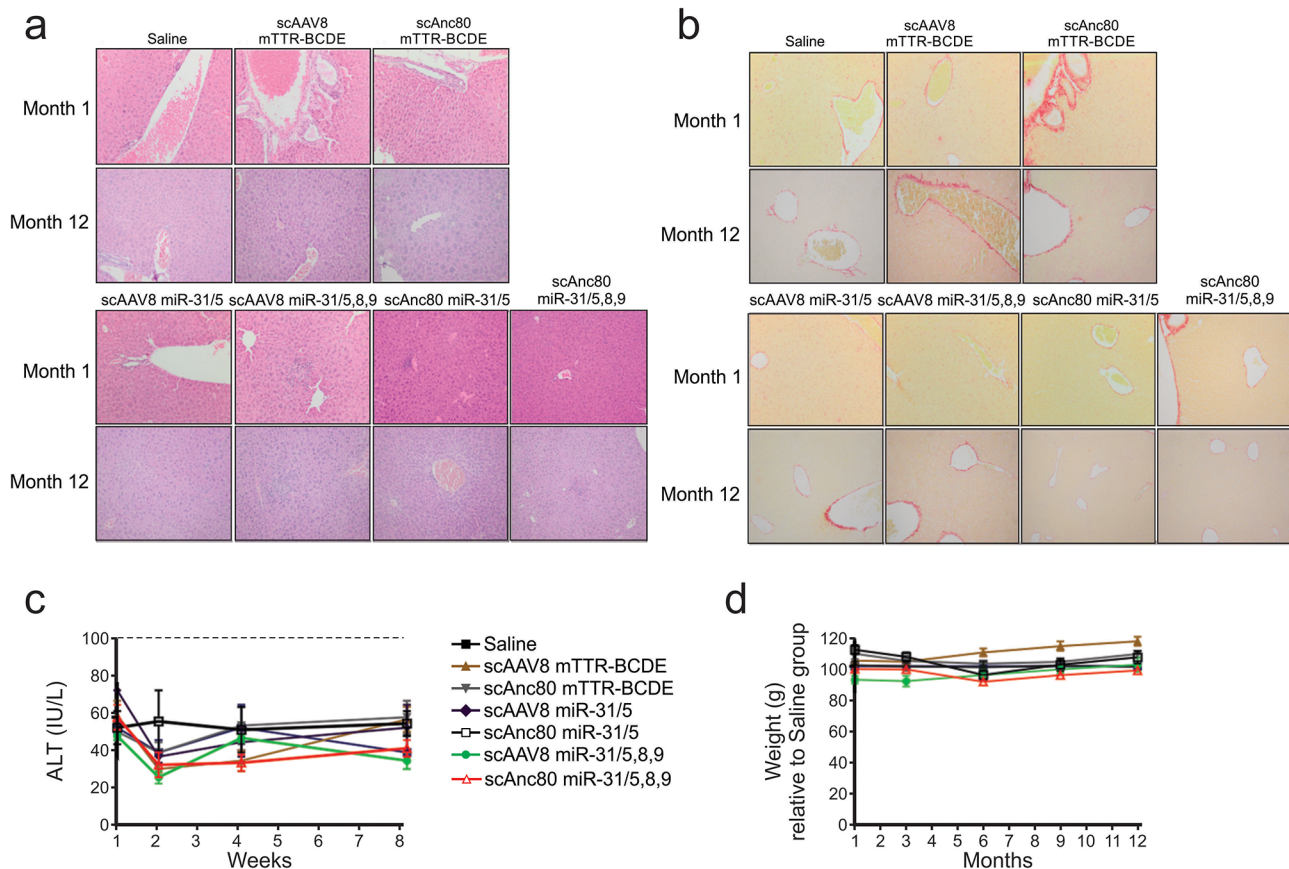


Fig. 6 Assessment of possible scAnc80-induced liver damage. Histochemical staining was performed using (a) H&E and (b) Sirius red on liver tissues obtained from 3 mice per group injected with saline or scAAVs. Arrows indicate areas of immune cell tissue infiltration. Mice were sacrificed at 1 or 12 months after scAAV administration and livers harvested. Representative low power fields are shown with scale bars of 200 μ m. The visualization of tissue was carried out at 40 \times magnification. **c.** Alanine aminotransferase (ALT) activity assay from murine serum samples. Serum was collected at weeks 1, 2, 4, and 8 after injection of groups of 3 mice with saline or scAAVs. The dashed line indicates the upper limit of normal ALT activity (100 IU/L). The means (\pm SEM) were derived from 3 mice per group. **d.** Evaluation of weight changes in HBV transgenic mice. The means (\pm SEM) were derived from 6 mice per group.

transgenic mice might be hepatotoxic, ALT activity was also measured. Similar ALT activities were observed in serum from mice receiving scAAVs or saline, and values were within the normal range (< 100 U/L) (Fig. 6c). Supporting absence of toxicity is the observation that body weights of mice were similar in groups of mice injected with scAAVs or saline (Fig. 6d). Moreover, all groups of mice maintained normal body weights and exhibited no signs of physiological distress.

Discussion

The current treatment regimen for chronic hepatitis B (CHB) has proven inadequate; hence, advancing more effective management is urgent to prevent serious complications. A gene therapeutic approach, adopted in this study, offers advantages to improve treatment of CHB. Earlier studies have demonstrated feasibility of inactivating HBV replication by repurposing the intrinsic RNAi pathway with exogenous synthetic miRs and expressed apri-miRs [22, 32, 42, 43]. To address issues related to

the safety and efficiency of delivering HBV-targeted gene silencing expression cassettes, we packaged DNA into an ancestral AAV. Using these scAnc80 vectors, efficient hepatotropic delivery of anti-HBV apri-miRs with sustained and significant inhibition of HBV gene expression were observed in cultured cells and in HBV transgenic mice over a 12 month period.

The mechanism behind the observed 12-month long silencing of HBV gene expression is interesting. Several studies have reported nonspecific integration of AAV genomes in vivo. Although the mechanism of integration is not understood, enhancer elements within the ITRs, promoter and 3' UTR regions have been implicated [44–47]. However, this is rare, especially with recent generation of AAVs lacking these enhancer elements. Formation of monomeric circular or polymeric circular concatemers of AAV genomes in host cells is well established [48–51]. Whereas the monomeric circular intermediates are short-lived, the high molecular weight concatemers are highly persistent and may account for the long-term therapeutic

efficacy observed in this study, as well as other investigations using animal models and clinical studies [52, 53]. Safety is an important consideration for developing therapy for use in humans. Adverse events have also recently been reported in larger animals following administration of a high AAV dose of 2×10^{14} viral particle equivalents per kilogram of body weight [54]. The study showed that high dose of AAVs caused physiological strain that necessitated sacrifice of a non-human primate as well as a pig. In previous studies, maximum cytokine concentrations were observed at 6 h post viral vector administration [55], hence we assessed the induction of inflammatory markers at 6 h post AAV injection. We showed here that administration of scAnc80 AAVs at doses that effectively suppressed HBV gene expression in vivo did not result in an obvious inflammatory response. Concentrations of each cytokine from a panel comprising IL-6, IL-10, IL-12p70, IFN- γ and TNF- α , were similar in mice receiving the scAnc80 vectors or saline. Assay of transcripts from genes associated with the IFN response, *IFIT-1*, *OAS-1* and *IFN- β* , corroborated the interpretation that the ancestral vectors did not induce an innate inflammatory response. Only MCP-1 was slightly elevated, but this could not be linked to scAnc80 infection specifically. Copregulation of IL-6 and IL-10 observed following a challenge by immunogenic poly I: C was not surprising. The role of IL-10 as an anti-inflammatory cytokine and its function to maintain homeostasis and avoid excessive tissue damage as a result of pro-inflammatory cytokine (e.g. IL-6) driven inflammation is well established [56–58]. Markers of inflammation based on histological analysis were also not linked to administration of scAnc80. Similarly, there was no evidence of fibrosis, based on Sirius red staining, in livers of mice receiving scAnc80 vectors. AAVs mediating RNAi activator expression have previously led to toxicity and death of mice, caused by saturation of Argonute-2, a mediator of the RNAi pathway. In these studies, AAVs bearing RNAi activator expression cassettes elevated ALT levels beyond normal range by 4 weeks and levels started to stabilize at ~week 6 [59–61]. In this study, administration of scAnc80 to induce RNAi-mediated silencing did not elevate ALT levels beyond the normal range. Although these data indicate that scAnc80 AAVs have a good safety profile, another factor limiting their toxicity is use of apri-miR as the antiviral sequences. Such Pol II expression cassettes have fewer toxic effects than Pol III short hairpin RNA cassettes [42, 59, 62].

AAVs are versatile vectors with varied tropism, their biosafety profile is well established and they are suitable for delivery of gene-based therapies in humans. Most importantly, ongoing efforts using different techniques based on directed evolution or rational design to alter the architecture of capsids led to development of AAV variants with good transduction efficiencies [63–66]. The

scAnc80 vectors are demonstrably safe to use, and capable of mediating a year-long suppression of HBV gene expression. An added useful feature of AAVs is that they infect HBV-replicating hepatocytes more efficiently than cells that do not contain the virus [67].

Since the *HBx* ORF is located immediately upstream of the single HBV transcription termination signal, targeting *HBx* results in silencing of all major HBV RNAs. The scAnc80 AAVs used in this study encoded monocistronic or polycistronic apri-miR with cognates at single or multiple coordinates within the *HBx* ORF. Disabling *HBx* has implications for expression of viral genes from cccDNA. Naturally, the Smc5/6 complex is antagonistic to transcription of extrachromosomal DNAs, such as cccDNA, and *HBx* promotes extrachromosomal transcription of cccDNA by enhancing degradation of the Smc5/6 complex [7]. Hence, a useful property of targeting *HBx*, as used here, is that the function of Smc5/6 should be restored with resultant suppression of viral gene expression from cccDNA. The HBV transgenic mice used in this study actively replicate HBV in hepatocytes and mimic chronic HBV infection in humans. However, drawbacks of the model are that HBV infection of murine hepatocytes does not occur and cccDNA is not produced [68]. Information regarding production of cccDNA by mice infected with AAVs carrying the HBV genome sequences (AAV-HBV) is contradictory and the mechanism by which the cccDNA is produced in these animals need further investigation [69–72]. However, the AAV-HBV model might be useful for evaluating efficacy of anti-HBV therapeutic candidates. Lack of data on HBeAg levels in cells or mice infected with scAAVs and the use of HBsAg assay with limited linear range are the limitations of this study. Nevertheless, the data show that exploiting the limited HBV genome plasticity and presence of *HBx* in all transcripts scAnc80 AAVs, these are useful properties that may be harnessed to treat HBV-infected individuals. Approaches combining RNAi activators and other anti-HBV agents may offer a more realistic approach in eliminating HBV [73]. A recent study using an AAV-HBV model has demonstrated a safe and a synergistic antiviral effect with clearance of the HBsAg when a lipid nanoparticle delivered siRNA targeting HBV consensus motifs was used in combination with IL-12 encoding mRNA. This study highlights the potential of RNAi and immunomodulatory approaches as a promising approach towards the development of CHB cure [74].

Although the evidence that Anc80L65 vectors can transduce primary human hepatocytes is lacking, and several AAV serotypes with proven human liver tropism such as AAV3 have been described [75], safety and efficiency of scAnc80 AAVs shown here reveals promise as a new type of vector. Our evidence supports their potential utility for treatment of chronic HBV infection. The task

ahead is to translate these findings to positive clinical outcomes for chronic HBV patients.

Supplementary Information

The online version contains supplementary material available at <https://doi.org/10.1186/s12985-025-02662-5>.

Supplementary Material 1

Author contribution

Conceptualization (M.B.M.); Data curation (N. M., S. L. and R. W.); Formal analysis (N. M.); Funding acquisition (P.A. and M.B.M.); Investigation (N. M.); Methodology (N. M, W.L. and A.E.); Resources (P.A.); Supervision (M.B.M. and P.A.); Writing – original draft (N.M.); Writing – review & editing (N. M., M.B.M., S. L., W.L, A.E. and R. W.).

Funding

Financial support from the South African National Research Foundation (Unique Grant Numbers: 118022 and 120383), South African Medical Research Council, Council for Scientific and Industrial Research (CSIR), Female Academic Leadership Fund and Carnegie/WITS University Enabling grant is gratefully acknowledged.

Data availability

No datasets were generated or analysed during the current study.

Declarations

Ethical approval

The use of HBV transgenic mice followed a protocol authorized by University of the Witwatersrand Animal Research and Ethics Committee (#2018/11/57/B, date of approval: 21/11/2018).

Competing interests

The authors declare no competing interests.

Received: 4 October 2024 / Accepted: 12 February 2025

Published online: 17 February 2025

References

1. WHO. Interim guidance for country validation of viral hepatitis elimination. WHO; 2021.
2. Ogunnaike M et al. Chronic Hepatitis B infection: New approaches towards Cure. *Biomolecules*. 2023. 13(8).
3. Zhu Y, et al. Kinetics of hepadnavirus loss from the liver during inhibition of viral DNA synthesis. *J Virol*. 2001;75(1):311–22.
4. Addison WR, et al. Half-life of the duck hepatitis B virus covalently closed circular DNA pool in vivo following inhibition of viral replication. *J Virol*. 2002;76(12):6356–63.
5. Naully PG, et al. cccDNA epigenetic regulator as target for therapeutical vaccine development against hepatitis B. *Ann Hepatol*. 2024;30(1):101533.
6. Tiollais P, Pourcel C, Dejean A. The hepatitis B virus. *Nature*. 1985;317(6037):489–95.
7. Decorsiere A, et al. Hepatitis B virus X protein identifies the Smc5/6 complex as a host restriction factor. *Nature*. 2016;531(7594):386–9.
8. Hanazaki K. Antiviral therapy for chronic hepatitis B: a review. *Curr Drug Targets Inflamm Allergy*. 2004;3(1):63–70.
9. van Nunen AB, et al. Is combination therapy with lamivudine and interferon-alpha superior to monotherapy with either drug? *Antiviral Res*. 2001;52(2):139–46.
10. Davidov Y, et al. Real-world hepatitis B antiviral treatment trends and adherence to practice guidelines: a large cohort study. *Acta Clin Belg*. 2023;78(4):291–7.
11. Wang F, et al. Role of hepatitis B virus non-structural protein HBx on HBV replication, interferon signaling, and hepatocarcinogenesis. *Front Microbiol*. 2023;14:1322892.
12. Sekiba K, et al. HBx-induced degradation of Smc5/6 complex impairs homologous recombination-mediated repair of damaged DNA. *J Hepatol*. 2022;76(1):53–62.
13. Li D, Hamadalnil Y, Tu T. Hepatitis B viral protein HBx: roles in viral replication and Hepatocarcinogenesis. *Viruses*. 2024. 16(9).
14. Carmona S, et al. Controlling HBV replication in vivo by intravenous administration of triggered PEGylated siRNA-nanoparticles. *Mol Pharm*. 2009;6(3):706–17.
15. Brzezinska J, et al. Synthesis of 2'-O-guanidinopropyl-modified nucleoside phosphoramidites and their incorporation into siRNAs targeting hepatitis B virus. *Bioorg Med Chem*. 2012;20(4):1594–606.
16. Marimani MD, et al. Inhibition of replication of hepatitis B virus in transgenic mice following administration of hepatotropic lipoplexes containing guanidinopropyl-modified siRNAs. *J Control Release*. 2015;209:198–206.
17. Yuen MF et al. Long-term serological, virological and histological responses to RNA inhibition by ARC-520 in Chinese chronic hepatitis B patients on entecavir treatment. *Gut*. 2022;71(4):789–97.
18. Mak LY et al. Long-term hepatitis B surface antigen response after finite treatment of ARC-520 or JNJ-3989. *Gut*. 2025;74:440–50.
19. Cideciyan AV et al. Human gene therapy for RPE65 isomerase deficiency activates the retinoid cycle of vision but with slow rod kinetics. 2008(1091–6490 (Electronic)).
20. Kassner U, et al. Gene Therapy in Lipoprotein Lipase Deficiency: Case Report on the first patient treated with Alipogene Tiparvovec under Daily Practice conditions. *Hum Gene Ther*. 2018;29(4):520–7.
21. Rangarajan S, et al. AAV5-Factor VIII gene transfer in severe Hemophilia A. *N Engl J Med*. 2017;377(26):2519–30.
22. Maepa MB, et al. Sustained inhibition of HBV Replication in Vivo after systemic injection of AAVs encoding Artificial Antiviral Primary MicroRNAs. *Mol Ther Nucleic Acids*. 2017;7:190–9.
23. Michler T, et al. Blocking sense-strand activity improves potency, safety and specificity of anti-hepatitis B virus short hairpin RNA. *EMBO Mol Med*. 2016;8(9):1082–98.
24. Zinn E, et al. Silico Reconstruction of the viral evolutionary lineage yields a potent gene therapy Vector. *Cell Rep*. 2015;12(6):1056–68.
25. Bourhill T. Successful disabling of the 5' UTR of HCV using adeno-associated viral vectors to deliver artificial primary microRNA mimics. University of the Witwatersrand: South Africa; 2015.
26. Nassal M. The arginine-rich domain of the hepatitis B virus core protein is required for pregenome encapsidation and productive viral positive-strand DNA synthesis but not for virus assembly. *J Virol*. 1992;66(7):4107–16.
27. Weinberg MS, et al. Specific inhibition of HBV replication in vitro and in vivo with expressed long hairpin RNA. *Mol Ther*. 2007;15(3):534–41.
28. Mnyandu N, Arbuthnot P, Maepa MB. Vivo delivery of cassettes encoding Anti-HBV primary MicroRNAs using an ancestral Adeno-Associated viral vector. *Methods Mol Biol*. 2020;2115:171–83.
29. McCarty DM, Monahan PE, Samulski RJ. Self-complementary recombinant adeno-associated virus (scAAV) vectors promote efficient transduction independently of DNA synthesis. *Gene Ther*. 2001;8(16):1248–54.
30. Grimm D, et al. Liver transduction with recombinant adeno-associated virus is primarily restricted by capsid serotype not vector genotype. *J Virol*. 2006;80(1):426–39.
31. Iwamoto M, et al. Evaluation and identification of hepatitis B virus entry inhibitors using HepG2 cells overexpressing a membrane transporter NTC1P. *Biochem Biophys Res Commun*. 2014;443(3):808–13.
32. Ely A, Naidoo T, Arbuthnot P. Efficient silencing of gene expression with modular trimeric Pol II expression cassettes comprising microRNA shuttles. *Nucleic Acids Res*. 2009;37(13):e91.
33. Crowther C, Mowa B, Arbuthnot P. Hepatic delivery of Artificial Micro RNAs using helper-dependent adenoviral vectors. *Methods Mol Biol*. 2016;1364:249–60.
34. Schinazi RF, Sommadossi JP, Rice CM, editors. A transgenic mouse lineage useful for testing antivirals targeting hepatitis B virus. *Frontiers in Viral Hepatitis*. Amsterdam, The Netherlands: Elsevier Science; 2003. pp. 197–202.
35. Schneider CA, Rasband WS, Eliceiri KW. NIH Image to ImageJ: 25 years of image analysis. *Nat Methods*. 2012;9(7):671–5.
36. Ellis BL, et al. A survey of ex vivo/in vitro transduction efficiency of mammalian primary cells and cell lines with nine natural adeno-associated virus (AAV1–9) and one engineered adeno-associated virus serotype. *Virology*. 2013;10:74.

37. Westhaus A, et al. High-throughput in Vitro, Ex vivo, and in vivo screen of Adeno-Associated Virus vectors based on physical and functional transduction. *Hum Gene Ther.* 2020;31(9–10):575–89.
38. Mowa MB, et al. Inhibition of hepatitis B virus replication by helper dependent adenoviral vectors expressing artificial anti-HBV pri-mirs from a liver-specific promoter. *Biomed Res Int.* 2014;2014:p718743.
39. Loomba R, et al. Discovery of Half-life of circulating Hepatitis B Surface Antigen in patients with chronic Hepatitis B infection using Heavy Water labeling. *Clin Infect Dis.* 2019;69(3):542–5.
40. Murray JM, Purcell RH, Wieland SF. The half-life of hepatitis B virions. *Hepatology.* 2006;44(5):1117–21.
41. Huang M, et al. Negative HBcAg in immunohistochemistry assay of liver biopsy is a predictive factor for the treatment of patients with nucleos(t)ide analogue therapy. *J Cell Mol Med.* 2018;22(3):1675–83.
42. Ely A, et al. Expressed anti-HBV primary microRNA shuttles inhibit viral replication efficiently in vitro and in vivo. *Mol Ther.* 2008;16(6):1105–12.
43. Ivacki D, et al. Sustained inhibition of hepatitis B virus replication in vivo using RNAi-activating lentiviruses. *Gene Ther.* 2015;22(2):163–71.
44. Nault JC, et al. Recurrent AAV2-related insertional mutagenesis in human hepatocellular carcinomas. *Nat Genet.* 2015;47(10):1187–93.
45. Chandler RJ, et al. Vector design influences hepatic genotoxicity after adeno-associated virus gene therapy. *J Clin Invest.* 2015;125(2):870–80.
46. Logan GJ, et al. Identification of liver-specific enhancer-promoter activity in the 3' untranslated region of the wild-type AAV2 genome. *Nat Genet.* 2017;49(8):1267–73.
47. -SRF, Chang LS, Chang Ls T, Fau, Shenk, Shenk T. A recombinant plasmid from which an infectious adeno-associated virus genome can be excised in vitro and its use to study viral replication. 1987(0022-538X (Print)).
48. Duan D, et al. Formation of adeno-associated virus circular genomes is differentially regulated by adenovirus E4 ORF6 and E2a gene expression. *J Virol.* 1999;73(1):161–9.
49. Duan D, et al. Circular intermediates of recombinant adeno-associated virus have defined structural characteristics responsible for long-term episomal persistence in muscle tissue. *J Virol.* 1998;72(11):8568–77.
50. Yang J, et al. Concatamerization of adeno-associated virus circular genomes occurs through intermolecular recombination. *J Virol.* 1999;73(11):9468–77.
51. Wang D, Tai PWL, Gao G. Adeno-associated virus vector as a platform for gene therapy delivery. *Nat Rev Drug Discov.* 2019;18(5):358–78.
52. Nathwani AC, et al. Long-term safety and efficacy of factor IX gene therapy in hemophilia B. *N Engl J Med.* 2014;371(21):1994–2004.
53. Nguyen GN, et al. A long-term study of AAV gene therapy in dogs with hemophilia A identifies clonal expansions of transduced liver cells. *Nat Biotechnol.* 2021;39(1):47–55.
54. Hinderer C, et al. Severe toxicity in Nonhuman Primates and piglets following high-dose Intravenous Administration of an Adeno-Associated Virus Vector Expressing Human SMN. *Hum Gene Ther.* 2018;29(3):285–98.
55. Crowther C, et al. Inhibition of HBV replication in vivo using helper-dependent adenovirus vectors to deliver antiviral RNA interference expression cassettes. *Antivir Ther.* 2014;19(4):363–73.
56. Iyer SS, Cheng G. Role of interleukin 10 transcriptional regulation in inflammation and autoimmune disease. *Crit Rev Immunol.* 2012;32(1):23–63.
57. Hacham M, et al. Interleukin-6 and interleukin-10 are expressed in organs of normal young and old mice. *Eur Cytokine Netw.* 2004;15(1):37–46.
58. Yanagawa Y, Iwabuchi K, Onoé K. Co-operative action of interleukin-10 and interferon-gamma to regulate dendritic cell functions. *Immunology.* 2009;127(3):345–53.
59. Giering JC, et al. Expression of shRNA from a tissue-specific pol II promoter is an effective and safe RNAi therapeutic. *Mol Ther.* 2008;16(9):1630–6.
60. Grimm D, et al. Fatality in mice due to oversaturation of cellular microRNA/short hairpin RNA pathways. *Nature.* 2006;441(7092):537–41.
61. Grimm D, et al. Argonaute proteins are key determinants of RNAi efficacy, toxicity, and persistence in the adult mouse liver. *J Clin Invest.* 2010;120(9):3106–19.
62. Boudreau RL, Martins I, Davidson BL. Artificial MicroRNAs as siRNA shuttles: Improved Safety as compared to shRNAs in vitro and in vivo. *Mol Ther.* 2008;17(1):169–75.
63. Deverman BE, et al. Cre-dependent selection yields AAV variants for wide-spread gene transfer to the adult brain. *Nat Biotechnol.* 2016;34(2):204–9.
64. Paulk NK, et al. Bioengineered AAV Capsids with Combined High Human Liver transduction in vivo and Unique Humoral Seroreactivity. *Mol Ther.* 2018;26(1):289–303.
65. Pekrun K, et al. Using a barcoded AAV capsid library to select for clinically relevant gene therapy vectors. *JCI Insight.* 2019;4(22):e131610.
66. Tse LV, et al. Structure-guided evolution of antigenically distinct adeno-associated virus variants for immune evasion. *Proc Natl Acad Sci U S A.* 2017;114(24):E4812–21.
67. Hosel M, et al. Hepatitis B virus infection enhances susceptibility toward adeno-associated viral vector transduction in vitro and in vivo. *Hepatology.* 2014;59(6):2110–20.
68. Guidotti LG, et al. High-level hepatitis B virus replication in transgenic mice. *J Virol.* 1995;69(10):6158–69.
69. Ko C et al. Intramolecular recombination enables the formation of hepatitis B virus (HBV) cccDNA in mice after HBV genome transfer using recombinant AAV vectors. *Antiviral Res.* 2021;194:105140.
70. Limani SW et al. In vivo modelling of Hepatitis B Virus Subgenotype A1 Replication using Adeno-Associated viral vectors. *Viruses.* 2021. 13(11).
71. Lucifora J, et al. Detection of the hepatitis B virus (HBV) covalently-closed-circular DNA (cccDNA) in mice transduced with a recombinant AAV-HBV vector. *Antiviral Res.* 2017;145:14–9.
72. Ye L et al. Adeno-Associated Virus Vector mediated delivery of the HBV Genome induces chronic Hepatitis B Virus infection and liver fibrosis in mice. *PLoS ONE.* 2015. 10(6).
73. van den Berg F et al. Advances with RNAi-Based therapy for Hepatitis B Virus infection. *Viruses.* 2020. 12(8).
74. Zai W, et al. Optimized RNA interference therapeutics combined with interleukin-2 mRNA for treating hepatitis B virus infection. *Signal Transduct Target Ther.* 2024;9(1):150.
75. Berns KI, Srivastava A. Next Generation of Adeno-Associated Virus vectors for Gene Therapy for Human Liver diseases. *Gastroenterol Clin North Am.* 2019;48(2):319–30.

Publisher's note

Springer Nature remains neutral with regard to jurisdictional claims in published maps and institutional affiliations.